3D Finite Elements for the Prediction of Complex Distortions in the Extrusion Blow Moulding Process

Debergue, Patricia; Laroche, Denis; Yousefi, Azizeh; DiRaddo, Robert; Atsbha, Haile

Publisher’s version / Version de l'éditeur:

PPS 2008: The Polymer Processing Society, 24th Annual Meeting [Proceedings], pp. 1-7, 2008

3D FINITE ELEMENTS FOR THE PREDICTION OF COMPLEX DISTORTIONS IN THE EXTRUSION BLOW MOULDING PROCESS

P. Debergue[1]*, D. Laroche[1], A.-M. Yousefi[1], R. DiRaddo[1] and H. Atsbha[2]

[1] *National Reseach Council of Canada, Industrial Materials Institute, 75 blvd de Mortagne, Boucherville, Quebec, J4B 6Y4, Canada – patricia.debergue@cnrc-nrc.gc.ca; denis.laroche@cnrc-nrc.gc.ca; azizeh.yousefi@cnrc-nrc.gc.ca; robert.diraddo@cnrc-nrc.gc.ca*

[2] *Kautex-Textron, Inc., Windsor (Ontario), Canada – haile.atsbha@kautex.textron.com*

Abstract – Finite element simulation of the blow moulding process has traditionally represented the parison with membrane or shell element formulations. In most cases the predicted wall thickness distribution corresponds well to the experimental measurements. However the thin membrane assumption may lead to poor predictions when applied to thick parison. It is also unable to represent the parison deformation when the level of distortion becomes elevated or complex, such as in the pinch-off area. In these areas, local parison compression, bending and shear require the use of three dimensional solid finite element formulations that provide the complex mechanical characteristics at elevated deformation levels. In this work, a solid brick finite element with displacement-based incompressible formulation is proposed for modelling large viscoelastic deformations of the parison during the clamping and inflation stages of the process. The parison formation was predicted based on the hybrid approach using a membrane model. The solid brick finite element mesh of the initial extruded parison was subsequently generated for the 3D part forming simulations. A K-BKZ viscoelastic model is used for representing the rheological behaviour of the parison deformation. This model is recognised for its ability to represent complex deformation modes of polymers. A multi-body contact algorithm for implicit finite element computation is used. It handles the contact between the parison and the mould as well as parison self contacts. Collisions between virtual nodes and surfaces moving with large displacement steps are detected with an implicit iterative approach that fully respects the non-penetration constraint. Special attention is being paid to the pinch-off area where complex parison distortions are encountered. This area is of particular interest for many industrial applications like fuel tanks. Numerical predictions are compared to experimental results as well as results obtained with the membrane formulation to justify the reliability of the proposed approach.

Introduction

Numerical process simulation is an important tool to assist in the development of complex blow moulded products. Finite element modelling using membrane or shell formulations has shown its ability to predict the consecutive stages of the process as a function of material properties and operating conditions [1]. The success of such integration was largely due to the use of temperature dependent viscoelastic material models capable of well describing the slow deformations of the parison swell and sag and the rapid inflation up to very high strain levels [2]. Among the various potential causes of imprecision in the process simulation is the modeling of the parison as a thin membrane. This assumption is justified by the fact that parisons are usually thin relative to their length and diameter. However the membrane formulation leads to poor accuracy in modeling thick parison deformations and complex distortions such as folding and local compression, particularly in the pinch-off area.

Recent papers have proposed the use of solid (3D) finite elements for modelling forming processes in order to overcome the limitations of the membrane (2.5D) approach [3, 4]. Mixed formulations with reduced selective integration for the pressure field were employed and gave satisfactory results when mesh refinement was used [4, 5]. Besides the elevated computational costs associated with this approach, difficulties regarding the incompressibility constraint and complex large deformations were highlighted. More recently, an incompressible 3D finite element formulation using an augmented Lagrange multiplier method was proposed [6-8]. This formulation helps solving the ill-conditioning problem associated with large distortions and incompressibility and therefore permits predictions of complex distortions of parisons. This formulation was used to integrate the parison sag, mould closing and parison inflation in consecutive simulation steps. Comparisons between the 2.5D and 3D approaches for simple geometries demonstrated the usefulness of the proposed 3D formulation.

Large deformations of relatively thin structures such as extruded parisons implicate non-linear deformation fields in the thickness direction. For this reason, proper prediction of parison deformation details requires high parison mesh refinement levels. The complexity of the deformation field becomes much more evident in the pinch area where the incompressible molten polymer is being squeezed. The pinch geometry in the mould surface mesh must be carefully treated. For these reasons, the application of 3D finite element simulation to complex industrial products is still a challenge. Costs and robustness of computations are the most limiting factors for the introduction of 3D simulations in the industry.

In this work, a 3D model for simulating extrusion blow moulding of complex industrial parts is presented. The finite element formulation uses an augmented Lagrange multiplier method to model large viscoelastic deformations of incompressible polymers. A multi-body contact algorithm that handles parison self-contacts in implicit finite element computation is introduced. Self-contacts are essential to properly capture complex deformations occurring in the pinch-off zone. In order to integrate parison swell, the initial 3D parison mesh is created using predicted diameter and thickness profile from an existing 2.5D software BlowParison® [9] developed at IMI. An experimental validation of the proposed integrated model is conducted on a plastic fuel tank. Simulations are performed with various mesh refinements in order to identify optimal mesh sizes with acceptable accuracy for the thickness predictions and for the pinch predictions. The validation work assesses the feasibility and reliability of using 3D finite elements on an industrial part. It also tries to demonstrate how 3D simulation can improve the results in zones of complex deformations like the pinch-off area.

3D Blow Moulding Model

Finite Element Formulation

In this work, a fully implicit 3D finite element formulation using the augmented Lagrange multiplier method is used [8]. The ill-conditioning problem of the penalty method is solved through the use of lower values of the penalty constant κ [10]. The solution for displacement and pressure is obtained from an iterative process where the pressure is updated locally at pressure points.

The selected element type is an 8 node brick isoparametric element with tri-linear Lagrangian approximation [11]. The element is a C_0 type and uses a total Lagrangian formulation with 8 Gauss integration points. The element has been successfully implemented for solving problems with quasi-incompressible materials. The incompressibility constraint is applied at a single pressure point, preserving the volume at the element level. The linear displacement field of the element has the major disadvantage of requiring a certain number of elements in the parison thickness direction to correctly represent the non-linearity of complex parison deformations. Compared to the higher order 27 node brick element that has already been successfully used for blow moulding and thermoforming applications [6-8], the 8 node brick is however less consuming in terms of calculation times and is therefore better suited for industrial applications.

Material Model

The rheological properties of the molten parison, defining the stress-strain relationship, are modelled with the K-BKZ constitutive equation [12, 13]. This viscoelastic model gives the true stresses σ at time t as a function of the Cauchy deformation c, strain invariants I_1 and I_2, memory function m, damping function h and the model constant θ.

$$\sigma = -q\mathrm{Id} + \frac{1}{1-\theta}\int_{-\infty}^{t} m(t-\tau)h(I_1, I_2)\left(c^{-1}(\tau,t) + \theta c(\tau,t)\right)d\tau \tag{1}$$

In this model heat transfer is not computed and the initial temperature profile after parison formation is considered uniform.

Parison Compression in the Pinch-area

Parison self contacts are modeled to predict material compression in the pinch zone. Contact algorithms are usually time consuming and limiting factors in complex finite element applications. They have been traditionally used in explicit software and include collision detection [14, 15], non-penetration constraint and friction/slip capabilities [16, 17]. In this work a multi-body contact algorithm for implicit finite element computation is proposed. Continuous collision detections between nodes and triangles are performed. The non-penetration constraint is handled through the use of a virtual contact mesh following the real finite element mesh as illustrated in Figure 1 [18]. Collisions between virtual nodes and surfaces moving with large displacement steps are detected in an iterative algorithm that preserves the non-penetration constraint. At every displacement increment, the new positions of the virtual nodes are computed as a minimization problem with the objective function F being their distance to the finite element mesh, subject to a non-penetration constraint g. The problem is given by Eqs. (2) and (3), with X_{Vi} and X_{FEi} being the positions of the virtual nodes and those of the finite element mesh, respectively.

$$F(X_{Vi}) = \sum_{i=1}^{N} |X_{Vi} - X_{FEi}| \tag{2}$$

$$g(X_{Vj}, X_{Vk}) = N_{Vk} \cdot (X_{Vk} - X_{Vj}) \leq 0 \tag{3}$$

Indices i represent all the surface nodes while j and k are for contacted nodes and surfaces, respectively. N_{Vk} and X_{Vj} are the virtual surface normal vector and the position of one of its connected nodes, respectively. Once contact is detected, it is handled with an augmented Lagrange algorithm. The technique is stable for large displacement increments and is therefore directly applicable to finite deformation analysis.

Figure 1 – Representation of the non-penetration constraint using a virtual contact mesh and a real finite element mesh.

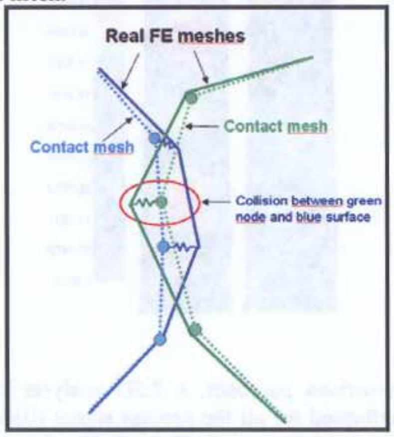

Parison Formation Model

The finite element software BlowParison® is based on a hybrid approach and a thin membrane assumption to predict die swell and resulting parison formation. The software couples a fluid mechanics approach to represent the die flow, with a solid mechanics approach to represent the parison behaviour outside the die [9]. The flow kinematics in the die is predicted based on the Hele–Shaw model, assuming Carreau rheological model type behaviour for the melt [19]. The particle tracking as well as the deformation prediction is performed using K-BKZ viscoelastic model (Eq. 1). The software includes die and parison programming, with input parameters close to machine parameters, to correctly represent the parison thickness profile and distribution. The effects of die design, operating conditions and resin characteristics are also taken into account. It has been successfully used in the past to model non-isothermal parison formation for several industrial parts, including fuel tanks [20, 21].

Experimental Validation

Experiments

The experimental validation was performed on an automotive fuel tank produced by Kautex Inc. The resin is a Basell Lupolen 4261A HDPE. The parts were blow moulded using a programmable diverging die on a continuous extrusion machine. The die gap opening control combined VWDS (Vertical Wall thickness Distribution System) and PWDS (Partial Wall thickness Distribution System) systems. A SFDR (Static Flexible Deformable Ring) system was also used to better control the circumferential wall thickness distribution, however this was not taken into account in the numerical modelling of the process. These controls provide high flexibility for optimizing the parison formation and consequently the part wall thickness distribution.

The processing conditions used for the fabrication of the fuel tank are summarized in Table 1. They result in a relatively thick parison with non-uniform blow ratios around the circumference of the part.

Table 1 – Processing conditions.

Extrusion stage	
Die diameter	222 mm
Flow rate	263 g/s
Extrusion time	52 s
Extrusion temperature	205 °C
Clamping and inflation stages	
Pinch-plates closing time	1 s
Pre-blow pressure / duration	0.0005 MPa / 0.4 s
Moulds closing time	1 s
Blow pressure / duration	0.03 MPa / 2 s

Figure 2 shows the fuel tank where wall thickness was measured. Parison length before mould closing and final part weight after deflashing, were also measured.

Figure 2 – Fuel tank showing wall thickness measurement locations.

Process Simulation

The rheological properties of the KBKZ constitutive model (Eq. 1) for the resin used in the simulations are given in Table 2.

Table 2 – Rheological properties of the Basell Lupolen 4261A HDPE.

Relaxation spectrum	
g_k (MPa)	**τ_k (sec)**
0.299897	0.006001
0.122096	0.035281
0.064703	0.207428
0.026908	1.219535
0.009207	7.170033
0.004831	42.154905
Non-linear terms	
α	16.0
β	0.1
θ	-0.11

Surface meshes for the mould halves and the part are shown in Figure 3. Details of the flash pockets, cutting edge and the compression zone are also illustrated.

Figure 3 – Part geometry and flash pockets of the mould surface model.

Simulation of the parison extrusion and formation using the membrane assumption were performed using the actual processing conditions. Figure 4 shows the predicted wall thickness distribution after parison formation. The clamping and inflation stages were simulated using a 3D parison mesh generated from these results.

Figure 4 – Predicted wall thickness distribution after parison formation.

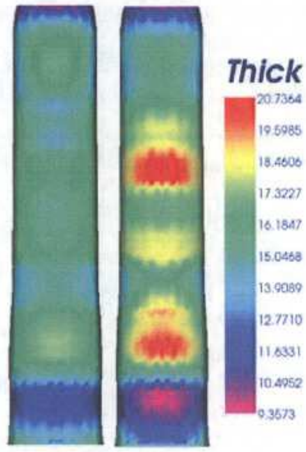

For comparison purposes, a 2.5D analysis has also been performed for all the process stages (BlowSim® software developed at IMI). Table 3 gives the predicted and measured parison length before mould closing as well as part weight after deflashing. This confirms the accuracy of the parison formation simulation. However the thickness distribution on the extruded parison was not experimentally validated.

Table 3 – Comparison of predicted and measured parison length before mould closing and part weight after deflashing.

	Measured	**Predicted**
Parison length (mm)	1440	1441
Part weight (kg)	9.7	10.2

For the 3D simulations, the number of elements was varied both through the thickness and on the surface in order to evaluate the effect of mesh refinement on prediction quality. Special attention is being paid to the pinch-off area where the number of elements through the thickness plays an important role. The parison meshes of the various simulations are described in Table 4.

Table 4 – Description of the parison meshes for the fuel tank analysis (NC = nber of nodes in the circumferential direction).

Case	**Parison mesh size (nb of nodes)**	**Nber of elements in the thickness (NET)**
3D NC=72	13536	1
3D NC=72	20304	2
3D NC=72	27072	3
3D NC=88	30360	2
3D NC=88	40480	3
2.5D NC=72	14688	-

Results and Discussion

Figure 5 illustrates 3D simulation results for the most refined case with 2 brick elements in the thickness direction (case '3D NC=88', NET=2). It shows the predicted wall thickness distribution (Figure 5a). Values were obtained by computing the shortest distance between the inner and outer parison surfaces. Details of the deformed mesh are also shown (Figure 5b). As it can be seen, process simulation using 3D elements provides a good representation of complex parison deformations, even close to the pinch-off area.

Figure 5 – 3D blow moulding simulation of the plastic fuel tank (a, b).

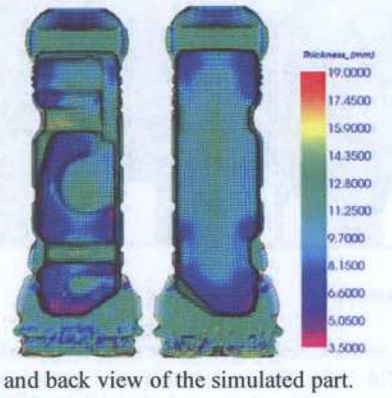

a) Front and back view of the simulated part.

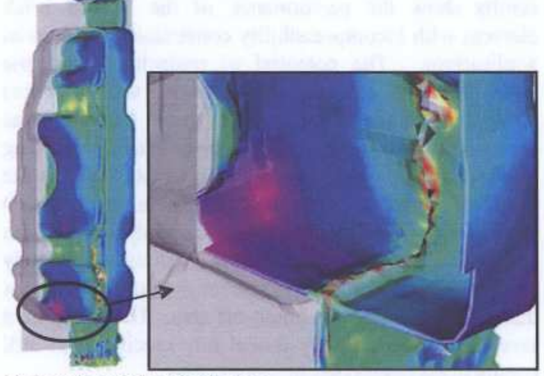

b) Details of the pinch area.

Figure 6 shows the comparison between measured and predicted wall thickness at several locations on the part. A 18% uniform thickness shrinkage was applied to account for density change due to cooling. Comparisons were done using the most refined case, referred to as '3D NC=88, NET=3' in Table 4. This 3D simulation tends to over predict the part thickness (around 10% thicker). However, considering the complexity of the die and parison programming, predictions compare reasonably well with the measurements. Qualitative observations during moulding showed a slight over prediction of the flash on the sides of the cavity. This could be due to an underestimation of the sag.

Figure 6 – Part thickness profile – Experimental results are shown in black; Simulation results are shown in red and in a white circle.

Wall thickness distributions along the circumference were extracted for two vertical positions. Figure 7 shows computed and measured values from the top front of the part where the geometry is non-uniform. Results from 2.5D simulations are also given. Simulations over predict thickness on the left side of the graph and under predict thickness on the right. However, both 2.5D and 3D simulations lead to acceptable thickness predictions.

Figure 7 – Thickness distribution around the circumference at the top front of the part.

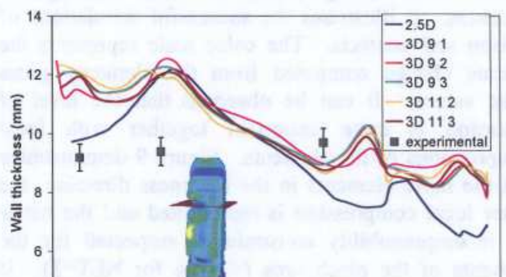

It can be observed that the difference between 2.5D and 3D predictions is increased in certain regions of the part, like corners, where material compression is neglected by the membrane elements. Also, the refinement level in the thickness direction has little effect on the predicted wall thickness. This effect is more pronounced in regions with abrupt geometry changes. Results also show that the use of 2 elements in the thickness direction is a minimum but probably enough. According to these results, increasing to 3 elements in the thickness does not provide significant improvements.

Figure 8 – Thickness distribution around the circumference in the centre back of the part.

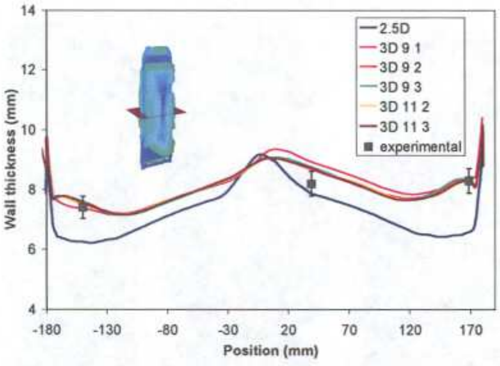

Figure 8 shows predicted and measured wall thickness around the circumference in the centre back of the part, where the geometry is the most uniform. Very good agreement between numerical predictions and experimental points for the 3D simulations are observed. The 2.5D simulations result in thinner part thickness in specific areas like corners, where the 3D simulations give better results. Clearly, the refinement level has nearly no effect and does not improve the thickness predictions. As for the top front of the part, 2 elements through the thickness are enough to obtain good predictions.

Figure 9 shows detailed views of the pinch-off area and results obtained using 1, 2 and 3 elements through the thickness. It illustrates the successful simulations of parison self contacts. The color scale represents the volume change computed from the elements gauss point values. It can be observed that the level of distortion is quite important together with local compressions of the elements. Figure 9 demonstrates that the more elements in the thickness direction, the better local compression is represented and the better the incompressibility constraint is respected for the elements of the pinch area (< 10% for NET=3). It highlights the advantage of using several elements in the thickness direction, for predicting local parison compression or severe distortion.

Figure 9 – Pinch-off detailed views using 1, 2 and 3 elements through the thickness. $J=V/V_0$ represents the volume change computed from the gauss point values.

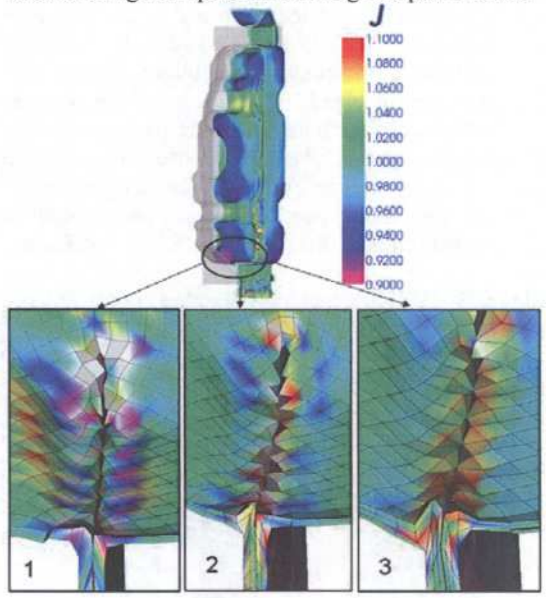

Conclusions

In this work an extrusion blow moulding model using 3D solid brick finite elements was presented. The model was validated on an industrial fuel tank. The results show the performance of the 8-node brick element with incompressibility constraint for industrial applications. The potential of replacing membrane with solid finite elements for improving wall thickness predictions when dealing with thick parisons was demonstrated. Clear advantages for enhancing predictions in particular zones of interests, such as the pinch or corners, where shown. In these areas 3D simulations could predict local material compression and high distortion. The use of a robust multi-body contact algorithm allowed to better predict the complex distortion arising in the pinch-off area. The refinement level needed to properly model this specific zone still results in elevated computational costs.

Acknowledgements

The authors wish to acknowledge the contribution of the members of the SIGBLOW group.

References (Times New Roman 10, bold)

1. D. Laroche et al., Polym. Eng. Sci., 1999, *39*, *7*, 1223.
2. A. Wineman, J. Non-Newtonian Fl. Mech., 1979, *6*, 111.
3. D. Laroche and F. Erchiqui, in Numiform '98 Proceedings, Balkema, 1998.
4. L.F. Menezes and C. Teodosiu, J. Mat. Proc. Tech., 2000, *97*, 100.

5. K.-D. Papoulia, Comput. Mech., 1999, *23*, 63.
6. P. Debergue and D. Laroche in ESAFORM 4 Proceedings, Liège, 2001.
7. P. Debergue and D. Laroche in ANTEC 2002 Proceedings, San Francisco, 2002, CD.
8. D. Laroche and P. Debergue in ANTEC 2002 Proceedings, San Francisco, 2002, CD.
9. A.M. Yousefi, P. Collins, S. Chang and R. DiRaddo, Polym. Eng. Sci., 2007, *47*, *1*, 1.
10. O.C. Zienkiewicz, J.P. Vilotte, S. Toyoshima and S. Nakazawa, Comp. Meth. App. Mech. Eng., 1985, *51*, 3.
11. G. Dhatt and G. Touzot, Une Présentation de la Méthode des Éléments Finis, Laval Univ. Press, Maloine S.A., 1981.
12. A. Kaye, *Non-Newtonian Flow Incompressible Fluids*, College of Aeronautics, Cransfield, Note No. 134, 1962.
13. B. Bernstein, E. Kearsley, and L.J. Zapas, Trans. Soc. Rheol., 1963, *7*, 391.
14. J.O. Hallquist, G.L. Goudreau, D.J. Benson, Comp. Meth. App. Mech. Eng., 1985, *51*, 107.
15. Z.H. Zhong, *Finite element procedures for contact-impact problems*, Oxford University Press, 1993
16. T.A. Laursen, J.C. Simo, Int. J. Num. Meth. Eng., 1993, *36*, 3451.
17. M.A. Puso, T.A. Laursen, Comp. Meth. App. Mech. Eng., 2004, *193*, 601.
18. R. Bridson et al. in ACM SIGGRAPH Proceedings, 2002.
19. C.L. Tucker III, *Computer Modeling for Polymer Processing – Fundamentals*, Hanser, New-York, 1989.
20. A.M. Yousefi, P. Collins, and R. DiRaddo in ANTEC 2003 Proceedings, Nashville, 2003, CD.
21. F. Thibault, A.M. Yousefi, R.W. DiRaddo and H. Atsbha in PPS 22 Proceedings, Yamagata, 2006, CD.